



*J. Serb. Chem. Soc.* 88 (12) 1319–1334 (2023)  
JSCS–5698

## Diorganotin(IV) complexes with hydroxamic acids derivatives of some histone deacetylases inhibitors

DANIJELA N. NIKOLIĆ<sup>1,2#</sup>, MARIJA S. GENČIĆ<sup>1\*</sup>, JELENA M. AKSIĆ<sup>1</sup>,  
NIKO S. RADULOVIĆ<sup>1#</sup>, DUŠAN S. DIMIĆ<sup>3#</sup> and GORAN N. KALUĐEROVIĆ<sup>2\*\*</sup>

<sup>1</sup>University of Niš, Faculty of Sciences and Mathematics, Department of Chemistry, Višegradska 33, 18000 Niš, Serbia, <sup>2</sup>University of Applied Sciences Merseburg, Department of Engineering and Natural Sciences, Eberhard-Leibnitz-Straße 2, DE-06217 Merseburg, Germany and <sup>3</sup>University of Belgrade, Faculty of Physical Chemistry, Studentski trg 12–16, 11000 Belgrade, Serbia

(Received 30 June, revised 18 July, accepted 8 September 2023)

**Abstract:** Organotin(IV) compounds show great potential as antitumor metal-lodrugs with lower toxicity and higher antiproliferative activity. Histone deacetylases (HDAC) inhibitors are characterised by high bioavailability and low toxicity. In this research, the two novel octahedral organotin(IV) complexes of physiologically active hydroxamate-based ligands, *N*-hydroxy-4-phenylbutanamide (**HL**<sub>1</sub>) and *N*-hydroxy-2-propylpentanamide (**HL**<sub>2</sub>), have been prepared and characterized using FTIR, <sup>1</sup>H-, <sup>13</sup>C- and <sup>119</sup>Sn-NMR spectroscopy. Particular emphasis was put on the binding characteristics of ligands. The structures were additionally analysed by the density functional theory at B3LYP-D3BJ/6-311++G(d,p)(H,C,N,O)/LanL2DZ(Sn) level. The theoretical IR and NMR spectra were compared to the spectroscopic data, and it was concluded that the predicted structures described well the experimental ones. The stability of different isomers of **HL**<sub>1</sub> and **HL**<sub>2</sub> was assessed by the natural bond orbital analysis, and the importance of intramolecular hydrogen bond was outlined. The interactions between donor atoms and Sn were investigated and correlated with the changes in chemical shift and the wavenumbers of characteristic vibrations.

**Keywords:** diphenyltin(IV); *N*-hydroxy-4-phenylbutanamide; *N*-hydroxy-2-propylpentanamide; spectral characterization; DFT; NBO.

\*\*\* Corresponding authors. E-mail: (\*)marija.gencic@pmf.edu.rs;

(\*\*)goran.kaluderovic@hs-merseburg.de

# Serbian Chemical Society member.

<https://doi.org/10.2298/JSC230630064N>

## INTRODUCTION

Histone deacetylases (HDACs) are key enzymes involved in the regulation of various physiological cellular processes, such as transcription, by catalysing the hydrolysis of the  $\epsilon$ -acetylated lysine chain in histones, but they are also being increasingly implicated in tumorigenesis. It is proven that HDAC inhibitors could elicit anticancer effects in tumour cells by their ability to impose cell cycle arrest, differentiation, DNA damage, autophagy, and/or apoptosis.<sup>1,2</sup> The traditional HDAC inhibitors are divided into four main groups: *i*) hydroxamic acids or hydroxamates, such as suberanilohydroxamic acid; *ii*) cyclic peptides, including depsipeptide; *iii*) benzamides, *e.g.*, chidamide; *iv*) short-chain fatty acids, including butyric, 4-phenylbutanoic and valproic acid (Fig. 1).<sup>2</sup> Previous studies have shown that combining the bioavailability and low toxicity of short-chain fatty acids with the bidentate binding ability of hydroxamates to the active site  $Zn^{2+}$  could be beneficial, resulting in analogues with enhanced potency (*e.g.*, *N*-hydroxy-4-phenylbutanamide) and/or altered HDAC isoform selectivity (*e.g.*, *N*-hydroxy-2-propylpentanamide).<sup>3,4</sup>

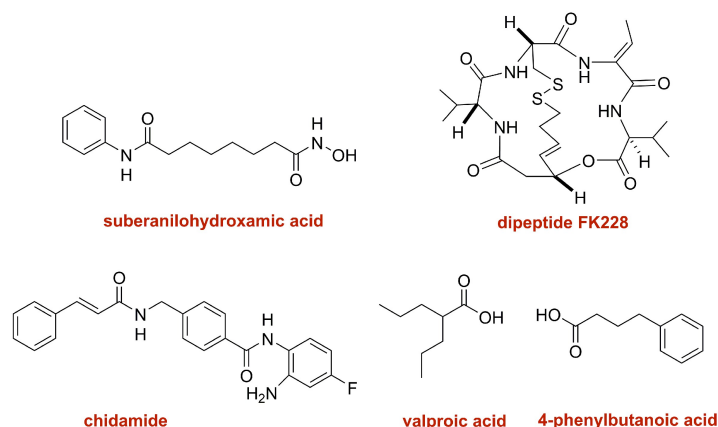


Fig. 1. Structures of HDAC inhibitors classes representatives.

Due to drug resistance, a broad spectrum of activity and toxicity-related issues of platinum-based antitumor chemotherapeutics, numerous efforts have been devoted to developing more effective non-platinum alternatives. Among them, organotin(IV) complexes have emerged as potential antitumor metallo-drugs due to lower toxicity, specifically targeted drug uptake by the cancerous cells, higher antiproliferative activity, and/or better excretion properties than platinum-based counterparts.<sup>5,6</sup> It has been shown that the number (mono-, di- or tri-) and type of alkyl/aryl groups linked to the central tin atom, the nature of the organic ligand, and the number of free coordination positions offered could play an

important role in the antiproliferative action of the organotin(IV) compounds.<sup>7</sup> A dozen of di- and tri-organotin(IV) complexes bearing different hydroxamic acids as ligands were prepared and structurally characterised recently, and it was discovered that some of them display potent cytotoxic and/or antimicrobial activities.<sup>2,8–10</sup> Tin compounds can also be used as photo-stabilizers for poly(vinyl chloride).<sup>11–13</sup>

Thus, this work deals with the preparation and characterization (FTIR, <sup>1</sup>H-, <sup>13</sup>C- and <sup>119</sup>Sn-NMR spectroscopy) of two new complexes **1** and **2** in which the known biologically active hydroxamate-based ligands, *N*-hydroxy-4-phenylbutanamide (**HL**<sub>1</sub>) and *N*-hydroxy-2-propylpentanamide (**HL**<sub>2</sub>), respectively, were combined with an diphenyltin(IV) moiety (Scheme 1). The structure and spectroscopic properties of compounds **1** and **2** were additionally confirmed by the quantum-chemical optimizations at B3LYP-D3BJ/6-311++G(d,p)(H,C,N,O)/LanL2DZ(Sn) level of theory. The intramolecular interactions governing the stability were analysed by the natural bond orbital theory.

#### EXPERIMENTAL AND THEORETICAL METHODS

##### *General methods*

All commercially available chemicals and solvents were used as purchased without further purification. Valproic acid was prepared *via* the standard malonate ester synthesis.<sup>14</sup> The identity and purity of the synthetic standard were confirmed by NMR and GC-MS analysis (trimethylsilyl derivative).

<sup>1</sup>H-NMR (400 MHz; including <sup>1</sup>H-NMR selective homonuclear decoupling experiments), <sup>13</sup>C-NMR, DEPT-90, DEPT-135, NOESY and gradient <sup>1</sup>H-<sup>1</sup>H COSY, HSQC and HMBC spectra were recorded on a Bruker Avance III 400 spectrometer (Bruker, Switzerland), while <sup>119</sup>Sn-NMR spectra were recorded on a Bruker Avance DRX 400 spectrometer. NMR spectra were measured at 25 °C in deuterated chloroform (CDCl<sub>3</sub>) and/or deuterated dimethyl sulfoxide (DMSO-*d*<sub>6</sub>). Chemical shifts ( $\delta$ ) given in ppm were referenced to tetramethylsilane (TMS) and/or residual non-deuterated/deuterated solvent peak as an internal standard. IR measurements (neat, attenuated total reflectance) were carried out on a Thermo Nicolet 6700 FTIR instrument (Waltham, USA) and the vibration frequencies are reported in wavenumbers (cm<sup>-1</sup>). The elemental analyses were carried out in a Vario EL III elemental analyser (Elementar Analysensysteme GmbH, Hanau, Germany) to determine C, H and N.

Analytical and spectral data of the synthesized compounds are given in Supplementary material to this paper.

##### *General procedure for preparation of hydroxamate ligand precursors*

A slightly modified previously published procedure was applied.<sup>15</sup> 4-Phenylbutanoic acid and valproic acid were converted to the corresponding acid chlorides by SOCl<sub>2</sub> and used without further purification. Et<sub>3</sub>N (19.5 mL, 0.14 mol) was added dropwise to precooled (0 °C) solution of NH<sub>2</sub>OH·HCl (9.7 g, 0.14 mol) in H<sub>2</sub>O (35.9 mL). Then the reaction mixture was stirred at 0 °C for 30 min, following the addition of the solution of acid chloride (7 mmol) in dry THF (14.4 mL). The reaction mixture was stirred for an additional 60 min and warmed to room temperature. Layers were separated and the aqueous solution was extracted with CH<sub>2</sub>Cl<sub>2</sub> (2×30 mL). The combined organic phases were dried with anhydrous MgSO<sub>4</sub> and

concentrated in *vacuo* to give the corresponding hydroxamic acid. *N*-hydroxy-4-phenylbutanamide (**HL**<sub>1</sub>) and *N*-hydroxy-2-propylpentanamide (**HL**<sub>2</sub>) were obtained as colourless crystals (in 34.5 and 45.7 % yield, respectively) and according to NMR analyses were sufficiently pure to be used further without purification (see Supplementary material). NMR data for ligands **HL**<sub>1</sub> and **HL**<sub>2</sub> were in general agreement with those previously reported.<sup>3,4</sup>

#### *General procedure for preparation of diphenyltin(IV) complexes*

A modified procedure by Li and co-workers (2004) was applied.<sup>2</sup> Typically, Ph<sub>2</sub>SnCl<sub>2</sub> (0.15 mmol) was added to the methanolic solution (3 mL) of the hydroxamic acid **HL**<sub>1</sub> or **HL**<sub>2</sub> (0.3 mmol) and KOH (0.3 mmol). The reaction mixture was stirred under N<sub>2</sub> at room temperature overnight. The white solid formed (KCl) was filtered off and the obtained filtrate was concentrated under a vacuum to yield the corresponding diorganotin(IV) complex.

#### *Theoretical methods*

The structures of ligands and organotin(IV) complexes were optimized in the Gaussian program package<sup>16</sup> by employing B3LYP-D3BJ<sup>17,18</sup> functional in conjunction with 6-311++G(d,p)<sup>19</sup> basis set for H, C, N and O, and LanL2DZ basis set for Sn.<sup>20,21</sup> The optimizations were performed without any geometrical constraints, and the absence of imaginary frequencies proved that the minima on the energy surface was found. The vibrational spectra were analysed and viewed in the Gauss View program.<sup>22</sup> The solvent environment was modelled by the conductor-like polarizable continuum (CPCM) model<sup>23</sup> for the measurements performed in chloroform and DMSO. The NMR spectra were predicted by the gauge independent atomic orbital approach (GAIO)<sup>24</sup> in the Gaussian Program package. The intramolecular interactions governing the stability of the ligand isomers and complexes were examined by the natural bond orbital (NBO) analysis.<sup>25</sup>

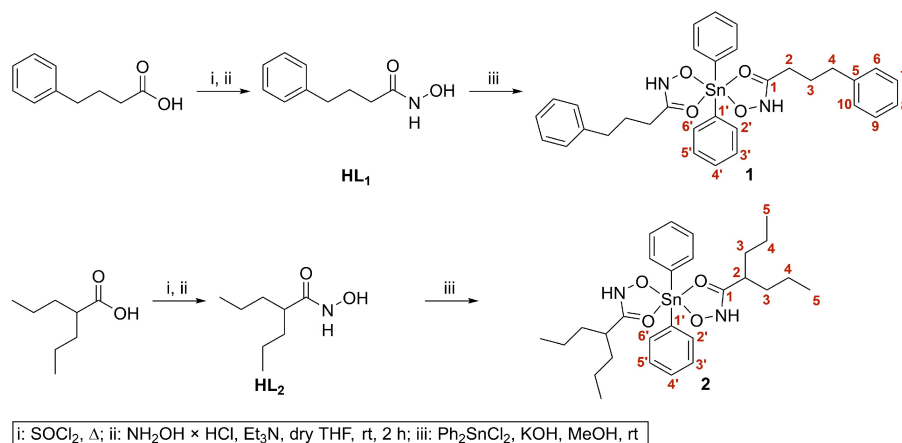
## RESULTS AND DISCUSSION

### *Synthesis and characterization*

The organotin(IV) hydroxamates **1** and **2** were prepared at room temperature by the reaction of one equivalent of Ph<sub>2</sub>SnCl<sub>2</sub> with two equivalents of ligand (**HL**<sub>1</sub> or **HL**<sub>2</sub>, respectively) in MeOH in the presence of an equimolar amount of KOH as a base (Scheme 1). Complexes **1** and **2** were obtained as colourless solids in very good yields and their purity was confirmed by C, H, and N elemental analysis. Compounds were further characterized by IR and multinuclear (<sup>1</sup>H-, <sup>13</sup>C- and <sup>119</sup>Sn-) NMR spectroscopy. The numbering of atoms in Scheme 1 was only used for NMR data assignment.

To investigate the vibrational modes of hydroxamic acids and how they change with complexation, the FTIR spectra of solid **HL**<sub>1</sub> and **HL**<sub>2</sub> and their organotin(IV) complexes **1** and **2**, respectively, were scanned in the range from 4500 to 400 cm<sup>-1</sup> (Figs. S-1–S-4). The ligand precursors showed the band at 3174 and 3176 cm<sup>-1</sup>, respectively, assigned to the N-H stretching vibrations, which was broader and less intense when they were complexed to a metal cation. The shift towards lower frequencies of the ν(C=O) from 1650 and 1627 cm<sup>-1</sup> in the ligand precursors **HL**<sub>1</sub> and **HL**<sub>2</sub> to 1596 and 1589 cm<sup>-1</sup> in complexes **1** and **2**, respectively, indicated that the ligand coordinates through oxygen atom. This

moderate to significant change in  $\nu(\text{C}=\text{O})$  vibration wavenumber could be indicative of the lengthening and weakening of the carbonyl bond.<sup>10</sup> The C–N stretching and N–H bending vibrations were found at  $1536\text{ cm}^{-1}$  in the **HL**<sub>2</sub> spectrum. Herein, the same vibrations were also influenced by the complexation, as it appeared as a broader band centred at  $1525\text{ cm}^{-1}$  in the corresponding organotin compound. The observed shifts are suggestive of bonding through carbonyl and hydroxamic oxygens (O,O coordination) and non-participation of nitrogen in bonding. Moreover, in the IR spectrum of complex **2** two additional bands at  $728$  and  $697\text{ cm}^{-1}$  that were not present in the spectrum of ligand precursor **HL**<sub>2</sub>, assigned as C–H wag and ring bend of the phenyl group, respectively, clearly indicated the introduction of Ph<sub>2</sub>Sn moiety in this molecule. New bands at about  $540\text{ cm}^{-1}$  (also not present in the ligand precursor) corresponding to  $\nu(\text{Sn}-\text{O})$  further confirm the formation of organotin(IV) complexes **1** and **2**, respectively.<sup>2</sup>



Scheme 1. Synthetic route to complexes **1** and **2**.

A comparison of <sup>1</sup>H- and <sup>13</sup>C-NMR spectra of diorganotin(IV) hydroxamates **1** and **2** with that of the ligand precursors (**HL**<sub>1</sub> and **HL**<sub>2</sub>, respectively) and of the starting material Ph<sub>2</sub>SnCl<sub>2</sub>, has further supported their formation. Hydroxamic acid **HL**<sub>1</sub> in CDCl<sub>3</sub> exhibited characteristic proton and carbon resonances for monosubstituted phenyl ring and three CH<sub>2</sub> groups belonging to propane-1,3-diyl fragment (Fig. 2, Figs. S-5 and S-6 of the Supplementary material). Alongside the mentioned resonances the two additional broad singlets corresponding to N–H and O–H protons, at 10.39 and 8.77 ppm, respectively, were observed in the <sup>1</sup>H-NMR spectrum (in DMSO-*d*<sub>6</sub>). The NMR spectra of the ligand precursor **HL**<sub>2</sub> were also recorded in both CDCl<sub>3</sub> and DMSO-*d*<sub>6</sub>. Among the aliphatic protons, the terminal methyl groups appeared as a triplet at 0.88 ppm ( $J^3 = 7.2\text{ Hz}$ ), while CH and CH<sub>2</sub> groups were observed as four complex multiplets (Fig. S-7 of

the Supplementary material) in  $\text{CDCl}_3$ . According to the interactions noted in the HSQC and  $^1\text{H}$ - $^1\text{H}$  COSY spectra the methylene groups in position 3 are anisochronous (Fig. 3A). These diastereotopic methylene groups exhibit a double magnetic nonequivalence: the two  $\text{CH}_2$  groups have different chemical shifts and the protons within them are nonequivalent as well and feature complex splitting patterns (*e.g.*, overlapping pairs of *ddd* or *ddt*). Therefore, it appears that a specific conformation around the  $\text{C}(2)\text{H}-\text{C}(3)\text{H}_2$  bond was preferred in ligand **HL**<sub>2</sub> leading to the magnetic nonequivalence of methylene groups. As expected, there were two methylene carbon signals in the  $^{13}\text{C}$ -NMR spectrum (at 34.83 and 20.80 ppm), along with one resonance for each of the carbonyl (at 174.47 ppm), methine (at 44.15 ppm), and methyl carbon (14.15 ppm) atoms (Fig. S-8 of the Supplementary material). In addition to four chemical shifts in the aliphatic region, the signals of the labile N-H and OH-protons were observed at 10.36 and 8.68 ppm, respectively, in  $^1\text{H}$ -NMR of ligand precursor in  $\text{DMSO}-d_6$  (Fig. S-9 of the Supplementary material).

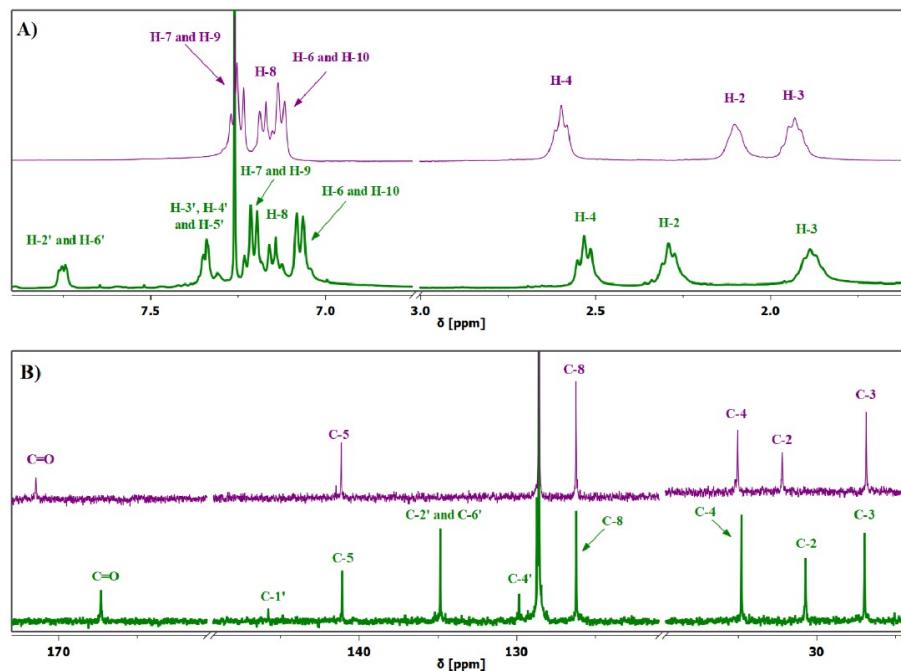


Fig. 2. Comparison of the  $^1\text{H}$ - (A) and  $^{13}\text{C}$ -NMR (B) spectra of ligand **HL**<sub>1</sub> (violet line) and complex **1** (green line) in  $\text{CDCl}_3$ .

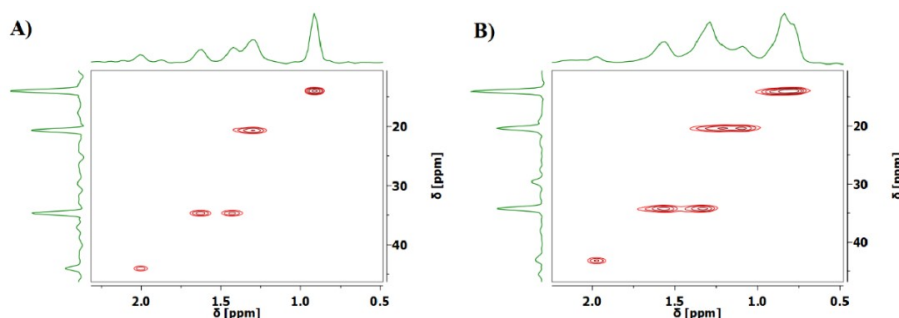


Fig. 3. Expansions of the aliphatic regions of HSQC spectra of ligand **HL**<sub>2</sub> (A) and complex **2** (B).

Despite their comprehensive chemistry and biology, the structures of hydroxamic acids in solution are still a matter of wide debate. If there is restricted rotation around the C–N bond then *Z* and *E* isomers should exist, while tautomerism could lead to the two additional enolic forms of hydroxamic acid (Fig. 4A).<sup>26</sup> The previous theoretical and NMR studies showed that primary hydroxamic acids tend to adopt the more stable keto-*E* and/or keto-*Z* conformations. Moreover, it was found that the prevalence of certain conformations strongly depends on concentration, temperature and the nature of the solvent.<sup>27</sup> Each of analysed ligands, **HL**<sub>1</sub> and **HL**<sub>2</sub>, showed a single set of characteristic resonances in both the <sup>1</sup>H- and <sup>13</sup>C-NMR spectra in DMSO-*d*<sub>6</sub> at room temperature (Figs. S-9 and S-10 of the Supplementary material), and this is consistent either with the presence of only one conformer (*E* or *Z*, due to the high rotational barrier) or a rapid interconversion between the two conformations, so that only one average set of signals is observed in the spectrum. Whatever the preferred conformation is, it is out of the question that hydroxamic acid must be in the prearranged keto-*Z* conformation in order to chelate the metal ion effectively. Thus clearly, the solvent in which metal complexation takes place (in our case methanol) has to play a crucial role in facilitating the required conformation changes necessary for (O,O) coordination.<sup>28</sup> Indeed, it is supposed that protic solvents, such as methanol, stabilize the keto-*Z* conformation by forming intermolecular hydrogen bonds (Fig. 4B).<sup>27</sup>

The appearance of characteristic chemical shifts of phenyl groups attached to the tin centre in the <sup>1</sup>H and <sup>13</sup>C spectra of complex **1** and **2** (in CDCl<sub>3</sub>), which were absent in the spectra of free ligands, clearly reveals the assimilation of the diphenyltin(IV) moiety (Figs. S-11–S-14 of the Supplementary material). Moreover, the carbonyl carbon (C=O) resonances that appeared at 170.73 and 174.47 ppm in the <sup>13</sup>C spectra of the hydroxamic acids, **HL**<sub>1</sub> and **HL**<sub>2</sub>, respectively, were shifted upfield in the corresponding complex (to 167.32 and 169.52 ppm, respectively), indicating an increase in electron density at the carbon atom when

the oxygen is chelated to the tin atom (Fig. 2B, Figs. S-12 and S-14). In complex **1**, this effect was also noted for  $\alpha$ -methylene carbon atom (C2, see Scheme 1;  $\Delta\delta = -0.76$ ), while in complex **2**, even the  $\delta$ -carbon atom (C5, see Scheme 1) experienced some marginal magnetic shielding ( $\Delta\delta$  in the range from  $-0.80$  to  $-0.05$  and gradually decreased with the distance from C=O group). In contrast, the resonances of all other carbon atoms in complex **1** were shifted downfield compared to the free ligand ( $\Delta\delta$  in the range from 0.46 to 0.82).

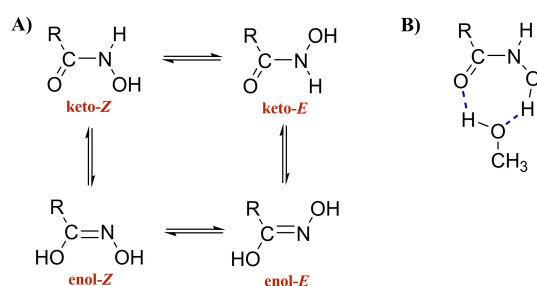


Fig. 4. Plausible conformations of a hydroxamic acid (A) and intramolecular H-bonding of hydroxamic acid in keto-Z conformation with methanol (B).

In the  $^1\text{H-NMR}$  spectra of **1** and **2** in  $\text{CDCl}_3$  also all the expected chemical shifts could be identified, with some evident coordination induced shifts in comparison to the appropriate ligand precursor (Fig. 2B, Figs. S-11 and S-13). In complex **1**, the methylene protons next to the hydroxamate C=O group (H-2), which are the closest to the coordination centre, were most notably shifted to higher frequencies ( $\Delta\delta = 0.18$ ). This deshielding of the H-2 protons may be attributed to the magnetic anisotropy of the phenyl and/or carbonyl groups (Fig. 2B). The complete assignments of the  $^1\text{H-}$  and  $^{13}\text{C-NMR}$  spectra of complex **1** in  $\text{CDCl}_3$  were achieved by a combination of data from DEPT,  $^1\text{H-}^1\text{H}$  COSY, NOESY, HMQC and HMBC spectra. The precise values of proton chemical shifts and coupling constants were determined using manual iterative full spin analysis (MestReNova 11.0.3–18688, Mestrelab Research, Santiago de Compostela, Spain). Unfortunately, the complete assignment of  $^1\text{H-NMR}$  data of complex **2** in  $\text{CDCl}_3$  was hampered by the fact that upon complexation of hydroxamic acid **HL**<sub>2</sub> the methylene groups in position 4 and methyl groups from *N*-hydroxy-2-propylpentanamide moiety became magnetically nonequivalent as well (Fig. 3B) and that some of the resonances originating from phenyl groups overlapped with the residual solvent signal. Therefore, the chemical shifts were estimated based on the observed HSQC interactions.

Finally, the tin chemical shift ( $^{119}\text{Sn}$ ) values often indicate the coordination number around the tin centre and, thus, provide valuable information about the geometry of organotin(IV) complexes.<sup>29</sup> In the  $^{119}\text{Sn-NMR}$  spectra of **1** and **2** (in

CDCl<sub>3</sub>; Figs. S-15 and S-16) one sharp signal (at  $-402.41$  and  $-349.95$  ppm, respectively) was present, which strongly supports the octahedral geometry of this tin(IV) complex.<sup>2,8</sup>

#### Theoretical analysis of ligands and complexes

The quantum-chemical methods were first employed to investigate the stability of different ligands **HL**<sub>1</sub> and **HL**<sub>2</sub> conformers to verify the experimental observation of the keto-*Z* isomer dominance. The optimized structures of ligands in vacuum are shown in Figs. 5 and S-17. Table I lists the electronic energies of the conformers calculated in vacuum relative to the most stable conformer.

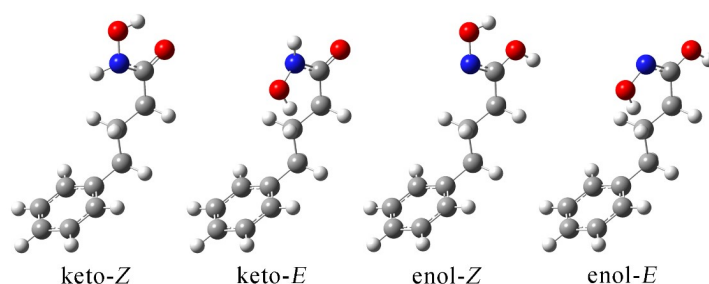


Fig. 5. Optimized isomers in vacuum (B3LYP-D3BJ/6-311++G(d,p) level of theory) of **HL**<sub>1</sub>.

TABLE I. Relative electronic and free energies (in kJ mol<sup>-1</sup>) to the most stable conformer (calculated at B3LYP-D3BJ/6-311++G(d,p) level of theory) for ligands **HL**<sub>1</sub> and **HL**<sub>2</sub>

Isomer	Electronic energies		Free energies	
	<b>HL</b> <sub>1</sub>	<b>HL</b> <sub>2</sub>	<b>HL</b> <sub>1</sub>	<b>HL</b> <sub>2</sub>
Keto- <i>Z</i>	0	0	0	0
Keto- <i>E</i>	4.5	9.1	4.1	9.8
Enol- <i>Z</i>	39.1	41.1	40.6	41.10
Enol- <i>E</i>	52.6	58.5	54.7	58.0

The results from Table I prove that the keto-*Z* isomers of both **HL**<sub>1</sub> and **HL**<sub>2</sub> were the most stable when both electronic and free energies were concerned. This result was expected due to the forming of the intramolecular hydrogen bond between the hydroxyl and carbonyl groups. The Second-order perturbation theory results, within NBO analysis, allowed the quantification of the stabilisation energy of this interaction.<sup>30</sup> The intramolecular hydrogen bonds, denoted as LP(O)→σ(O-H), had energies of 17.8 (**HL**<sub>1</sub>) and 19.7 kJ mol<sup>-1</sup> (**HL**<sub>2</sub>). Higher stabilization energy in the case of the second hydroxamic acid ligand was probably due to the positive inductive effect of heptane-4-yl moiety, while in the case of **HL**<sub>1</sub>, the electron density is distributed through the phenyl group and hydroxylamide parts. Another important stabilisation interaction is LP(N)→π(C=O),

with 76.4 and 61 kJ mol<sup>-1</sup> stabilization energies for **HL**<sub>1</sub> and **HL**<sub>2</sub>, respectively. This interaction represents charge delocalisation within the amide group. The other reason for the preferability of this isomer is the formation of the intermolecular hydrogen bonds with solvent molecules and the lowest steric hindrance, as previously discussed in the experimental part. Once the rotation around the N atom occurred, the keto-*E* isomers were formed. These conformers do not contain intramolecular hydrogen bond, and the stabilisation energies originating from LP(N)→π(C=O) are lower for several kJ mol<sup>-1</sup>. The rotational barriers of 4.5 and 9.1 kJ mol<sup>-1</sup> are still sufficiently low to allow the presence of a keto-*E* isomer in the solution. The formation of a double bond between carbon and nitrogen atom made the system much more rigid. In the case of enol-*Z* isomers, the intramolecular hydrogen bond is formed. Due to the system's rigidity, the distance between the hydrogen atom donor and acceptor in hydrogen bond is much longer than in keto-*Z* isomers leading to lower stabilisation energies of 7.3 (**HL**<sub>1</sub>) and 7.9 kJ mol<sup>-1</sup> (**HL**<sub>2</sub>). The stabilization of enol-*E* isomers is the lowest compared to the other three in both ligands.

The applicability of the chosen level of theory for the optimisation of ligand structures was further examined by comparing the experimental and the theoretical IR and NMR spectra. The most prominent bands of N–H and O–H stretching vibrations of structures optimised in vacuum were around 3624 (3174 in experimental spectrum, N–H) and 3561 cm<sup>-1</sup> (O–H). Lower wavenumber for the N–H stretching vibration results from the intramolecular hydrogen bond formation. These values were significantly higher than those experimentally observed because the experimental spectra were recorded in the solid sample, while the optimizations were performed on an isolated molecule in vacuum.<sup>31</sup> Due to the intermolecular interactions, the wavenumbers shift to lower values. On the other hand, the C=O stretching vibrations were observed at 1663 (**HL**<sub>1</sub>) and 1661 cm<sup>-1</sup> (**HL**<sub>2</sub>) for the structures optimized in vacuum. These values reproduce well the experimental ones considering all of the optimization limitations (1647 and 1627 cm<sup>-1</sup> in experimental spectra, respectively). The C–N stretching and N–H bending vibrations were found at 1557 cm<sup>-1</sup> in the spectra of both **HL**<sub>1</sub> and **HL**<sub>2</sub>, which is several cm<sup>-1</sup> higher than in the experimental spectrum (1541 and 1536 cm<sup>-1</sup>).

When NMR spectra are concerned, Table II lists the experimental and theoretical values of the chemical shifts of **HL**<sub>1</sub>, while the analogous table for **HL**<sub>2</sub> is presented in the Supplementary material. The experimental and theoretical chemical shifts were compared by calculating the correlation coefficient (*R*) and the mean absolute error (*MAE*). The theoretical shifts were obtained for the structures optimised in chloroform. The calculated chemical shifts were overestimated, and the correction factors were determined from the dependency between experimental and theoretical values. These factors were 0.95 and 0.94 for <sup>1</sup>H-

and  $^{13}\text{C}$ -NMR spectra of **HL**<sub>1</sub>. The calculated values show a high  $R$  value and low  $MAE$  (0.14 ( $^1\text{H}$ -NMR) and 2.4 ppm ( $^{13}\text{C}$ -NMR)), proving the reproducibility of the experimental data. The lowest values of the chemical shifts in  $^1\text{H}$ -NMR spectra were obtained for the hydrogen atoms of the aliphatic chain between 1.93 and 2.60 ppm in the experimental and between 1.51 and 2.53 ppm in the theoretical spectrum. As expected, the chemical shifts of hydrogen atoms attached to aromatic carbon atoms were in a narrow range. The largest discrepancies between the experimental and the theoretical data were calculated for the hydrogen atoms attached to oxygen and nitrogen atoms ( $>1.5$  ppm) due to the formation of stabilisation interactions with the solvent molecules. When  $^{13}\text{C}$ -NMR chemical shifts are concerned, the values for carbon atoms of the aromatic ring were almost equal, because the similarity of the chemical environment of carbon atoms was not significantly influenced by the present aliphatic chain. The similar results was obtained for ligand **HL**<sub>2</sub>.

TABLE II. Experimental and theoretical (at B3LYP-D3BJ/6-311++G(d,p) level of theory) of **HL**<sub>1</sub>

$^1\text{H}$ Chemical shifts, ppm			$^{13}\text{C}$ Chemical shifts, ppm		
H atom	Experimental	Theoretical	C atom	Experimental	Theoretical
C3-H	1.93	1.51	C3	26.1	30.8
C2-H	2.10	2.44	C2	31.5	37.5
C4-H	2.60	2.53	C4	34.3	39.8
C6-H	7.13	7.50	C8	125.5	125.0
C10-H	7.13	7.50	C6	127.9	127.5
C8-H	7.18	7.50	C10	127.9	127.4
C7-H	7.25	7.69	C7	127.9	127.7
C9-H	7.25	7.50	C9	127.9	127.7
O-H	8.77	7.18	C5	140.4	143.3
N-H	10.39	7.85	C1	170.7	166.8
$R$		0.993	$R$		0.995
$MAE$ / ppm		0.14	$MAE$ / ppm		2.4

Once the reproducibility of experimental spectral data was shown, it could be concluded that the optimized structures represented well the structures in solution. The same methodology was applied for the structural analysis of complexes **1** and **2**. The optimized structures are given in Fig. 6, although other conformers could also possibly exist. The complexation occurs through two oxygen atoms and Sn as the central metal ion. The ligands are positioned symmetrically around the Sn ion. The bond distances between deprotonated hydroxyl group oxygen and Sn were, on average, 2.20 Å, while between the carbonyl oxygen and Sn were 2.29 Å. The optimised structure also supported the experimental finding that a bond was not formed between Sn and the nitrogen atom. The NBO analysis gave the stabilisation energies formed between oxygen atoms and Sn. In

the case of complex **1**, the stabilisation interactions between hydroxyl group oxygen and Sn had an energy of  $222 \text{ kJ mol}^{-1}$ , and between the carbonyl oxygen and Sn,  $180 \text{ kJ mol}^{-1}$ . These energies explained the difference in the bond lengths between Sn and O atoms. The stronger interactions were formed between **HL**<sub>2</sub> and Sn ( $\text{LP}(\text{O}_{\text{hydroxyl}}) \rightarrow \text{LP}(\text{Sn})$  ( $266 \text{ kJ mol}^{-1}$ ) and  $\text{LP}(\text{O}_{\text{carbonyl}}) \rightarrow \text{LP}(\text{Sn})$  ( $133 \text{ kJ mol}^{-1}$ )). The electron density is mostly localised on the hydroxylamide group, as previously explained for the isolated ligand.

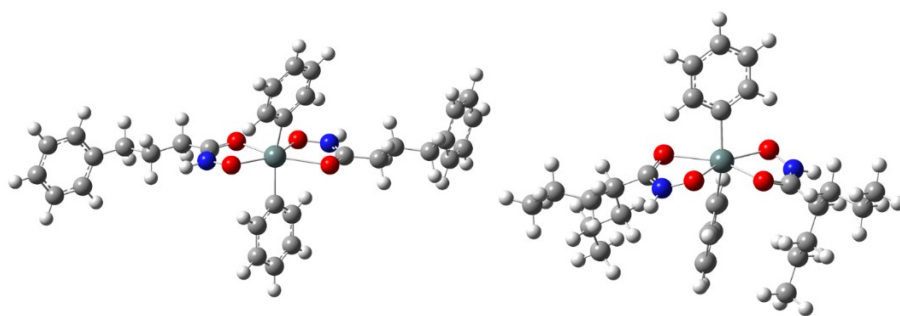


Fig. 6. Optimized structures (at B3LYP-D3BJ/6-311++G(d,p)(H,C,N,O)/LanL2DZ(Sn) of complexes **1** (left) and **2** (right).

Upon the complexation, the characteristic frequencies of the groups included in the compound formation were changed as experimentally observed. The C=O stretching vibration wavenumber lowered to  $1610$  (**HL**<sub>1</sub>) and  $1598 \text{ cm}^{-1}$  (**HL**<sub>2</sub>) in the theoretical spectra of compounds optimised in vacuum ( $1596$  and  $1589 \text{ cm}^{-1}$  in experimental spectra). The difference of around  $50 \text{ cm}^{-1}$ , due to the formation of the complex, was equal in the experimental and predicted spectra. The same was observed for the C–N stretching and N–H bending vibrations. In the lower part of the theoretical spectrum, a band at  $546 \text{ cm}^{-1}$  assigned to  $\nu(\text{Sn–O})$  was obtained, similar to the experimental spectrum ( $540 \text{ cm}^{-1}$ ), as an important finding to support the formation of organotin(IV) complexes **1** and **2**.

The experimental and the theoretical NMR spectra of complexes **1** and **2** were also compared. Tables III and S-II list the experimental and theoretical chemical shifts in chloroform. The correlation coefficients between experimental and theoretical values are 0.995 for both <sup>1</sup>H- and <sup>13</sup>C-NMR spectra of complex **1**, with MAE values being 0.11 and 2.1 ppm, respectively. A shift in values was observed for the carbonyl oxygen ( $166.8$  ppm in the spectrum of **HL**<sub>1</sub> and  $163.9$  ppm in a spectrum of complex **1**), thus proving that this group is included in the complex formation, as it is experimentally confirmed. Similar was observed for **HL**<sub>2</sub> and complex **2**. Change in chemical shift of C2 of  $1.8$  ppm was also induced upon complexation. The rest of the values remained almost the same (for example,  $\delta(\text{C5})$  was found to be  $143.3$  (**HL**<sub>1</sub>) and  $143.8$  ppm (**1**)).

Based on the comparison between the experimental and the theoretical IR and NMR spectra of complexes **1** and **2**, it can be concluded that the predicted structure from Scheme 1 was confirmed.

TABLE III. Experimental and theoretical (at B3LYP-D3BJ/6-311++G(d,p) level of theory) of complex **1**

<sup>1</sup> H chemical shifts, ppm			<sup>13</sup> C chemical shifts, ppm		
H atom	Experimental	Theoretical	C atom	Experimental	Theoretical
C3-H	1.89	1.46	C3	27.0	31.3
C2-H	2.28	2.23	C2	30.7	35.7
C4-H	2.53	2.43	C4	34.8	39.8
C6-H	7.07	7.17	C8	126.2	125.5
C10-H	7.07	7.17	C7	128.6	128.4
C8-H	7.15	7.12	C9	128.6	128.3
C7-H	7.22	7.22	C6	128.6	127.9
C9-H	7.22	7.22	C10	128.6	127.9
C4'-H	7.34	7.22	C3'	128.7	127.8
C3'-H	7.35	7.22	C5'	128.7	127.0
C5'-H	7.35	7.22	C4'	129.9	128.4
C2'-H	7.75	7.85	C2'	134.9	134.0
C6'-H	7.75	7.98	C6'	134.9	135.1
<i>R</i>		0.995	C5	141.1	143.8
<i>MAE</i> / ppm		0.11	C1'	145.8	150.9
			C1	167.3	163.9
			<i>R</i>		0.995
			<i>MAE</i> / ppm		2.1

#### CONCLUSION

The two new diphenyltin(IV) complexes of biologically active hydroxamate-based ligands, *N*-hydroxy-4-phenylbutanamide (**HL**<sub>1</sub>) and *N*-hydroxy-2-propylpentanamide (**HL**<sub>2</sub>), have been synthesised and characterized by IR, <sup>1</sup>H-, <sup>13</sup>C- and <sup>119</sup>Sn-NMR spectroscopies. The bonding through hydroxamic and carbonyl oxygens (O,O coordination mode) has been indicated by the presence of characteristic bands in the IR spectra. The six-coordinate octahedral geometry around tin has been proposed based on <sup>119</sup>Sn-NMR data. All the expected chemical shifts were present in the <sup>1</sup>H- and <sup>13</sup>C-NMR spectra of complexes **1** and **2**. Some evident coordination-induced shifts could be noted compared to the ligand precursors. The complete assignments of the <sup>1</sup>H- and <sup>13</sup>C-NMR spectra of complex **1** in CDCl<sub>3</sub> were achieved by combining the data from 2D NMR spectra and <sup>1</sup>H-NMR simulation. The relative stability of different conformers of **HL**<sub>1</sub> and **HL**<sub>2</sub> was explained through the intramolecular hydrogen bond formation and LP(N)→→π(C=O) stabilisation interaction. The theoretical IR and NMR spectra of the ligands reproduced well the experimental results. The structure optimisation of complexes **1** and **2** proved the binding mode through the oxygen atoms, with

stronger bonds formed with hydroxyl oxygen (shorter bond and higher stabilization interaction energy) than with carbonyl oxygen. The changes in IR spectra upon complexation were successfully modelled by quantum-chemical calculations. High values of correlation coefficient ( $>0.991$ ) and low mean absolute error values for comparing the experimental and the calculated NMR chemical shifts proved the predicted structure. Further studies on biological activity of herein described complexes are to be performed, having in mind the well-known biological potential of both ligands and Sn.

#### SUPPLEMENTARY MATERIAL

Additional data and information are available electronically at the pages of journal website: <https://www.shd-pub.org.rs/index.php/JSCS/article/view/12461>, or from the corresponding author on request.

*Acknowledgments.* The work was supported by the Ministry of Science, Technological Development and Innovation of Serbia (contract number: 451-03-47/2023-01/200124 and 451-03-47/2023-01/200146). This research is a part of Danijela N. Nikolić's PhD Thesis supervised by Marija S. Genčić. D.D. wishes to express his gratitude to Filip Vlahović, PhD, for his generous help with the optimization of organotin(IV) compounds.

#### ИЗВОД

#### ДИОРГАНОКАЛАЈ(IV) КОМПЛЕКСИ СА ХИДРОКСАМАТНИМ ДЕРИВАТИМА КИСЕЛИНА КРАТКОГ НИЗА КОЈЕ ПРЕДАСТАВЉАЈУ НДАС ИНХИБИТОРЕ

ДАНИЈЕЛА Н. НИКОЛИЋ<sup>1,2</sup>, МАРИЈА С. ГЕНЧИЋ<sup>1</sup>, ЈЕЛЕНА М. АКСИЋ<sup>1</sup>, НИКО С. РАДУЛОВИЋ<sup>1</sup>,  
ДУШАН С. ДИМИЋ<sup>3</sup> и ГОРАН Н. КАЛУЂЕРОВИЋ<sup>2</sup>

<sup>1</sup>Универзитет у Нишу, Природно-математички факултет, Департаман за хемију, Вишеградска 33, 18000 Ниш, <sup>2</sup>University of Applied Sciences Merseburg, Department of Engineering and Natural Sciences, Eberhard-Leibnitz-Straße 2, DE-06217 Merseburg, Germany и <sup>3</sup>Универзитет у Београду, Факултет за физичку хемију, Студентски тир 12–16, 11000 Београд

Органокалајна(IV) једињења показују велики значај као антитуморски металолективи са ниском токсичношћу и изразитом антипролиферативном активношћу. Инхибиторе хистон деацетилазе карактеришу велика биодоступност и ниска токсичност. У овом раду је описана синтеза и карактеризација (FTIC, <sup>1</sup>H-, <sup>13</sup>C- и <sup>119</sup>Sn-NMR спектроскопија) два нова комплекса дифенилкалаја(IV) са биолошки активним хидроksamатним лигандима, *N*-хидрокси-4-фенилбутанамидом (**HL**<sub>1</sub>) и *N*-хидрокси-2-пропилпентанамидом (**HL**<sub>2</sub>). Посебна пажња је посвећена предвиђању начина везивања лиганда у добијеним комплексима. Структуре су додатно испитане применом теорије функционала густине на B3LYP-D3BJ/6-311++G(d,p)(H,C,N,O)/LanL2DZ(Sn) нивоу. Теоријски IC и NMR спектри су упоређени са спектроскопским подацима и закључено је да предвиђене структуре добро описују експерименталне. Стабилност различитих изомера **HL**<sub>1</sub> и **HL**<sub>2</sub> је испитана теоријом природних орбитала и приказан је значај интрамолекуларске водоничне везе. Интеракције између доносних атома и Sn су испитане и корелисане са променом у хемијским померањима и таласним бројевима карактеристичних вибрација.

(Примљено 30. јуна, ревидирано 18. јула, прихваћено 8. септембра 2023)

## REFERENCES

1. J. Chen, D. Faller, R. Spanjaard, *Curr. Cancer Drug Targets* **3** (2003) 219 (<https://doi.org/10.2174/1568009033481994>)
2. G. Li, Y. Tian, W.-G. Zhu, *Front. Cell Dev. Biol.* **8** (2020) (<https://doi.org/10.3389/fcell.2020.576946>)
3. J. L. Tischler, B. Abuaita, S. C. Cuthpert, C. Fage, K. Murphy, A. Saxe, E. B. Furr, J. Hedrick, J. Meyers, D. Snare, A. R. Zand, *J. Enzyme Inhib. Med. Chem.* **23** (2008) 549 (<https://doi.org/10.1080/14756360701715703>)
4. D. M. Fass, R. Shah, B. Ghosh, K. Hennig, S. Norton, W.-N. Zhao, S. A. Reis, P. S. Klein, R. Mazitschek, R. L. Maglathlin, T. A. Lewis, S. J. Haggarty, *ACS Med. Chem. Lett.* **2** (2011) 39 (<https://doi.org/10.1021/ml1001954>)
5. J. Devi, M. Yadav, D. K. Jindal, D. Kumar, Y. Poornachandra, *Appl. Organomet. Chem.* **33** (2019) 1 (<https://doi.org/10.1002/aoc.5154>)
6. S. N. Syed Annuar, N. F. Kamaludin, N. Awang, K. M. Chan, *Front. Chem.* **9** (2021) (<https://doi.org/10.3389/fchem.2021.657599>)
7. S. Hadjikakou, N. Hadjiliadis, *Coord. Chem. Rev.* **253** (2009) 235 (<https://doi.org/10.1016/j.ccr.2007.12.026>)
8. X. Shang, E. C. B. A. Alegria, M. F. C. Guedes da Silva, M. L. Kuznetsov, Q. Li, A. J. L. Pombeiro, *J. Inorg. Biochem.* **117** (2012) 147 (<https://doi.org/10.1016/j.jinorgbio.2012.08.019>)
9. S. Kumari, N. Sharma, *J. Coord. Chem.* **72** (2019) 584 (<https://doi.org/10.1080/00958972.2019.1573993>)
10. V. K. Choudhary, A. K. Bhatt, N. Sharma, *J. Coord. Chem.* **72** (2019) 372 (<https://doi.org/10.1080/00958972.2019.1573993>)
11. N. Naom, E. Yousif, D. S. Ahmed, B. M. Kariuki, G. A. El-Hiti, *Polymers* **14** (2022) 4590 (<https://doi.org/10.3390/polym14214590>)
12. R. R. Arraq, A. G. Hadi, D. A. Ahmed, G. A. El-Hiti, B. M. Kariuki, A. A. Husain, M. Bufaroosha, E. Yousif, *Polymers* **15** (2023) 550 (<https://doi.org/10.3390/polym15030550>)
13. R. Haddad, S. Khadum, M. Ali, A. Majeed, A. Husain, M. Bufaroosha, D. Ahmed, E. Yousif, *Bull. Chem. Soc. Ethiop.* **37** (2023) 771 (<https://dx.doi.org/10.4314/bcse.v37i3.18>)
14. M. S. Genčić, N. M. Stojanović, M. Z. Mladenović, N. S. Radulović, *Neurochem. Int.* **161** (2022) 105433 (<https://doi.org/10.1016/j.neuint.2022.105433>)
15. U. Gravemann, J. Volland, H. Nau, *Neurotoxicol. Teratol.* **30** (2008) 390 (<https://doi.org/10.1016/j.ntt.2008.03.060>)
16. <http://www.gaussian.com>
17. A. D. Becke, *Phys. Rev., A* **38** (1988) 3098 (<https://doi.org/10.1103/PhysRevA.38.3098>)
18. A. D. Becke, E. R. Johnson, *J. Chem. Phys.* **123** (2005) 154101 (<https://doi.org/10.1063/1.2065267>)
19. T. H. Dunning, *J. Chem. Phys.* **90** (1989) 1007 (<https://doi.org/10.1103/1.456153>)
20. P. J. Hay, W. R. Wadt, *J. Chem. Phys.* **82** (1985) 299 (<https://doi.org/10.1063/1.448975>)
21. P. J. Hay, W. R. Wadt, *J. Chem. Phys.* **82** (1985) 270 (<https://doi.org/10.1063/1.448799>)
22. *Gauss View, Version 5*, Semichem Inc., Shawnee, KS, 2009
23. A. V. Marenich, C. J. Cramer, D. G. Truhlar, *J. Phys. Chem., B* **113** (2009) 6378 (<https://doi.org/10.1021/jp810292n>)
24. J. A. Bohmann, F. Weinhold, T. C. Farrar, *J. Chem. Phys.* **107** (1997) 1173 (<https://doi.org/10.1063/1.474464>)

25. J. P. Foster, F. Weinhold, *J. Am. Chem. Soc.* **102** (1980) 7211 (<https://doi.org/10.1021/ja00544a007>)
26. D. A. Brown, W. K. Glass, R. Mageswaran, S. A. Mohammed, *Magn. Reson. Chem.* **29** (1991) 40 (<https://doi.org/10.1002/mrc.1260290109>)
27. B. García, S. Ibeas, J. M. Leal, F. Secco, M. Venturini, M. L. Senent, A. Niño, C. Muñoz, *Inorg. Chem.* **44** (2005) 2908 (<https://doi.org/10.1021/ic049438g>)
28. D. A. Brown, R. A. Coogan, N. J. Fitzpatrick, W. K. Glass, D. E. Abukshima, L. Shiels, M. Ahlgrén, K. Smolander, T. T. Pakkanen, T. A. Pakkanen, M. Peräkylä, *J. Chem. Soc., Perkin Trans.* **2** (1996) 2673 (<https://doi.org/10.1039/P29960002673>)
29. J. Adeyemi, D. Onwudiwe, *Molecules* **23** (2018) 2571 (<https://doi.org/10.3390/molecules23102571>)
30. D. S. Dimić, Z. S. Marković, L. Saso, E. H. Avdović, J. R. Đorović, I. P. Petrović, M. J. Stanisavljević, D. D. Stevanović, I. Potočňák, E. Samoľová, S. R. Trifunović, J. M. Dimitrić Marković, *Oxid. Med. Cell. Longev.* **2019** (2019) 2069250 (<https://doi.org/10.1155/2019/2069250>)
31. T. Eichhorn, F. Kolbe, S. Mišić, D. Dimić, I. Morgan, M. Saoud, D. Milenković, Z. Marković, T. Ruffer, J. Dimitrić Marković, G. N. Kaluderović, *Int. J. Mol. Sci.* **24** (2023) (<https://doi.org/10.3390/ijms24010689>).